ResearchGate

See discussions, stats, and author profiles for this publication at: https://www.researchgate.net/publication/327930868

Decentralized Composite Adaptive Control for Friction Compensation in Collective Transport with No Feedback on Payload Motion

Conference Paper · September 2018

CITATIONS
0

READS
38

2 authors:

Hamed Farivarnejad
Arizona State University
6 PUBLICATIONS **21** CITATIONS

SEE PROFILE

Spring M. Berman
Arizona State University
54 PUBLICATIONS **636** CITATIONS

SEE PROFILE

Some of the authors of this publication are also working on these related projects:

Project Design and control of stochastic behavior of swarms of robots View project

Project Control of Adaptive Robotic Swarms in Inaccessible Environments View project

All content following this page was uploaded by Hamed Farivarnejad on 28 September 2018.

The user has requested enhancement of the downloaded file.

Decentralized Composite Adaptive Control for Friction Compensation in Collective Transport with No Feedback on Payload Motion

Hamed Farivarnejad and Spring Berman

Abstract— **In this paper, we propose a decentralized composite adaptive controller for planar collective transport by a team of point-mass robots that are rigidly attached to a payload, whose motion is influenced by Coulomb and viscous friction. The controller only requires the robots' measurements of their own velocities. The robots have no knowledge about the magnitude and direction of the friction forces, and the only information provided to them is the target speed and direction of transport. Moreover, the robots have no knowledge about the team size, the distribution of the teammates around the payload, and the payload's linear and angular velocities. We prove that the closed-loop system with the proposed controller is globally stable, and that the payload's motion converges to the target velocity. In addition, the payload's angular velocity is driven to zero, and its drift from the desired path is considerably reduced when the number of robots is increased. We validate the analytical results for our control strategy with simulations of collective transport by teams of two different sizes. The simulations demonstrate that the size of the team has a significant effect on the smoothness of the payload's motion, its rate of convergence to the target transport velocity, and its drift from the desired path.**

I. Introduction

Potential applications of cooperative payload manipulation by multi-robot systems include construction, manufacturing, assembly in space and underwater, search-and-rescue operations, and disaster response. Many of these scenarios will take place in uncertain, GPS-denied environments with unreliable communication. In such scenarios, decentralized control strategies with limited data and communication and provable guarantees on performance will be needed to reliably achieve manipulation objectives. In this paper, we propose an approach to this problem that is inspired by the phenomenon of group food retrieval in ants [1], [2], [3]. This behavior is an example of decentralized cooperative manipulation in which the transport teammates do not follow predefined trajectories, use explicit communication, or have prior information about the payload, number and distribution of teammates around it, locations of obstacles, and the magnitudes and directions of disturbances in the environment. Although the ants know the direction to their nest, their actions during collective transport are likely influenced only by their locally perceived information.

Our work in this paper extends our previous decentralized control strategy for collective transport in [4] to account for the effect of external disturbances to the system in the form of friction forces and moments. We consider a team of identical point-mass robots that move on a planar surface and are rigidly attached to a payload in an arbitrary configuration, as shown in Figure 1. We assume that the robots do not have global localization or communication capabilities, and they lack information about the payload dynamics, the number of robots in the transport team, and the robots' distribution around the payload. Subject to these constraints, we design a fully decentralized adaptive controller such that the robots use only local measurements to compensate for the effects of Coulomb and viscous friction on the payload. Despite the robots' lack of information about the magnitudes and directions of the friction forces, the controller drives the robot team to transport the payload to a goal location along a straight path at a regulated velocity. We assume that each robot knows the target direction to the goal and the desired transport speed and can measure its own velocity. The design of this controller constitutes an effort toward multi-robot implementation of ant-like collective transport strategies that are robust to different types of payloads and environments.

Other decentralized control strategies for cooperative manipulation have previously been proposed for scenarios that are not subject to all of these constraints. These strategies, many of which apply to a team of robots with identical sensing and actuation capabilities, are designed to improve the system's robustness to errors, failures, and disturbances. In the decentralized approach proposed in [5], robots push a large payload to a goal when their line of sight to the goal is occluded by the payload. In other approaches, robots communicate their measurements to each other in order to estimate unknown parameters of the payload [6], [7]. In more recent work [8], robots jointly reach the same desired motion by running a time-varying quadratic program which is solved online by a neural network scheme. Other approaches do not require inter-robot communication or prior information about the payload dynamics [9], but they rely on a supervisor to define the robot and payload trajectories beforehand [10], [11], [12]. In [13], a strategy inspired by formation control is presented for a flexible payload that requires regulation of contact forces.

Recently, adaptive robust control approaches have been proposed for planar and three-dimensional manipulation. These approaches combine a stabilizing term with a regression term in the controller in order to achieve stabilization in presence of parameter uncertainties. However, the approaches require either prior information about the robots' distribution around the payload or feedback on the payload's

This research was supported by ONR Young Investigator Award N00014-16-1-2605.

Hamed Farivarnejad and Spring Berman are with the School for Engineering of Matter, Transport and Energy, Arizona State University (ASU), Tempe, AZ 85287, USA {Hamed.Farivarnejad, Spring.Berman}@asu.edu

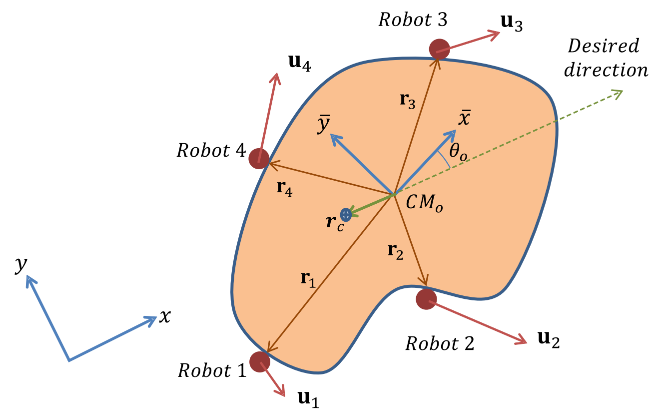

Fig. 1. Illustration of a collective transport team with four point-mass robots and the associated coordinate systems.

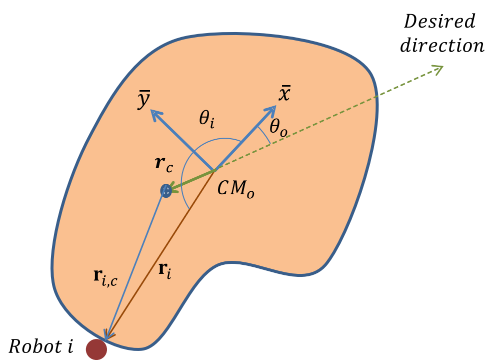

Fig. 2. Illustration of the geometric parameters that express the position of a robot in the local coordinate frame of the load.

motion. [14], [15], [16], [17], [18], [19], [20]. In [21], a decentralized approach is proposed for cooperative manipulation in which the robots use an adaptive controller to compensate for the effect of friction and have a common reference model for the desired motion. Whereas this approach requires the robots to have access to measurements of the payload's linear and angular velocities, ours does not require any information on the payload's motion. The controller that we present here is based on the proportional-integral (PI) controller in our previous work [4], where we analytically proved the asymptotic convergence of the system to the target transport velocity and zero drift from the desired path. To this PI controller, we add an adaptive control law that estimates the effect of Coulomb and viscous friction forces on the payload and is updated by a decentralized composite adaptation law, which uses two different sources to extract information about the unknown parameters: tracking error and prediction error. We prove the global stability of the system and the boundedness of the estimation errors using Lyapunov's direct method. We validate our control approach with numerical simulations.

II. Dynamical Model

We consider a payload that is transported by N point-mass robots, as shown in Figure 1. We assume that the payload is in contact with the ground during transport. The dynamical model of the entire system, including both the load and the robots, is given by the model that we derived in [4], [22] with the addition of constant disturbances in the form of Coulomb and viscous friction on the load.

We define m as the mass of the entire system and J as the system's moment of inertia about the axis that is normal to the plane of the load's motion and passes through the system's center of gravity. The inertial reference frame is fixed such that the x-axis points in the target direction of transport. We define the position of the system's center of mass in the inertial reference frame as $\boldsymbol{x}_o = [x_o \ y_o]^T \in \mathbb{R}^2$ and the load's orientation in this frame as θ_o. We will use $\boldsymbol{q}_o = [x_o \ y_o \ \theta_o]^T \in \mathbb{R}^3$ as generalized coordinates that describe the motion of the entire system. As shown in Figure 2, $\boldsymbol{r}_i = [r_{ix} \ r_{iy}]^T \in \mathbb{R}^2$ denotes the vector from the system's center of mass to the attachment point of robot i in the inertial frame, and θ_i denotes the angle of this vector in a local coordinate frame that is fixed to the load. Each robot i applies an actuating force $\boldsymbol{u}_i = [u_{ix} \ u_{iy}]^T \in \mathbb{R}^2$ to the payload. We denote the vector of all applied forces by $\boldsymbol{u} = \left[(\boldsymbol{u}_1)^T \cdots (\boldsymbol{u}_N)^T\right]^T \in \mathbb{R}^{2N}$. We denote the Coulomb friction force, viscous friction force, and viscous friction moment on the load by $\boldsymbol{f}_f \in \mathbb{R}^2$, $\boldsymbol{f}_v \in \mathbb{R}^2$, and $M_v \in \mathbb{R}$, respectively. These friction forces and moment are defined according to the model derived in [23]:

$$\boldsymbol{f}_f = -\mu_f mg \boldsymbol{e}_{\dot{\boldsymbol{x}}_o}, \ \boldsymbol{f}_v = -\mu_v \dot{\boldsymbol{x}}_o, \ M_v = -\mu_v \frac{J}{m} \dot{\theta}_o, \quad (1)$$

where g is the magnitude of gravitational acceleration, $\boldsymbol{e}_{\dot{\boldsymbol{x}}_o}$ is the unit vector along the velocity of the system's center of mass, and μ_f and μ_v are the Coulomb and viscous friction coefficients, respectively. As stated in [23], the effect of the Coulomb friction on the rotational motion of the load can be neglected (i.e., there is no Coulomb frictional moment).

The equation of motion of the system is then given by:

$$\begin{bmatrix} m\boldsymbol{I} & 0 \\ 0 & J \end{bmatrix} \ddot{\boldsymbol{q}}_o = \begin{bmatrix} \boldsymbol{I} & \cdots & \boldsymbol{I} \\ \hat{\boldsymbol{r}}_1 & \cdots & \hat{\boldsymbol{r}}_N \end{bmatrix} \boldsymbol{u} + \begin{bmatrix} \boldsymbol{f}_f + \boldsymbol{f}_v \\ M_v \end{bmatrix}, \quad (2)$$

in which $\boldsymbol{I} \in \mathbb{R}^{2\times 2}$ is the identity matrix and $\hat{\boldsymbol{r}}_i = [-r_{iy} \ r_{ix}] \in \mathbb{R}^{1\times 2}$.

III. Controller Design

In this section, we present decentralized robot controllers for the system described by Equation (2) that produce asymptotic convergence to desired transport characteristics in the presence of Coulomb and viscous friction on the load. The control objectives for the robot team are: (1) to transport the load without rotation along a target direction at a desired speed v_{des}; that is, to ensure that the load's linear and angular velocities obey $\lim_{t\to\infty} \dot{\boldsymbol{q}}_o(t) = [v_{des} \ 0 \ 0]^T$, and (2) to eliminate the load's drift from the desired path, defined as the line between the initial and target positions of its center of mass. Toward this end, we modify the controller in our previous work [4] by adding two decentralized adaptive terms that compensate for the effects of Coulomb and viscous friction during transport.

Coulomb friction has a constant magnitude and a slowly time-varying direction for smooth courses of collective transport that do not undergo sharp changes in the direction of the transport velocity. Since adaptive controllers are designed for systems with unknown constant parameters, but usually produce satisfactory performance even when the parameters vary slowly over time [24], we define an adaptive controller under the assumption that Coulomb friction acts as a constant disturbance to the system. In addition, we model the viscous friction forces according to Equation (1) as functions of the unknown coefficient μ_v, and we design the corresponding adaptive term in the controller to estimate this coefficient.

A. Control Law and Closed-Loop Dynamics

We define $\dot{\boldsymbol{x}}_i = [\dot{x}_i \; \dot{y}_i]^T \in \mathbb{R}^2$ as the velocity of robot i with respect to the inertial frame. Defining $s_{ix} := (\dot{x}_i - v_{des})$ and $s_{iy} := \dot{y}_i$, we denote the *velocity error* of robot i by $\boldsymbol{s}_i := [s_{ix} \; s_{iy}]^T \in \mathbb{R}^2$. The vector $\hat{\boldsymbol{a}}_{if} := [\hat{a}_{ifx} \; \hat{a}_{ify}]^T \in \mathbb{R}^2$ is the estimate by robot i of the Coulomb friction, which is assumed to be a constant disturbance on the load as discussed above. Robot i also estimates the viscous friction coefficient, μ_v, as $\hat{a}_{iv} \in \mathbb{R}$. We define the control law for robot i as:

$$\boldsymbol{u}_i = -\boldsymbol{K}\boldsymbol{s}_i - \boldsymbol{K}_I \int_o^t \boldsymbol{s}_i d\tau + \hat{\boldsymbol{a}}_{if} + \hat{a}_{iv}\dot{\boldsymbol{x}}_i, \tag{3}$$

where $\boldsymbol{K} = k\boldsymbol{I} \in \mathbb{R}^2$ and $\boldsymbol{K}_I = k_I\boldsymbol{I} \in \mathbb{R}^2$ are diagonal positive definite matrices containing the controller gains.

Using this control law for each robot, we now describe the closed-loop dynamics of the system. We model the fraction of the actual Coulomb and viscous friction that acts on each robot i as:

$$\begin{aligned} \boldsymbol{a}_{if} &= \epsilon_{if}\boldsymbol{f}_f, \quad \sum_{i=1}^{N} \epsilon_{if} = 1, \\ a_{iv} &= \epsilon_{iv}\mu_v, \quad \sum_{i=1}^{N} \epsilon_{iv} = 1. \end{aligned} \tag{4}$$

The estimation errors $\tilde{\boldsymbol{a}}_{if} \in \mathbb{R}^2$ and $\tilde{a}_{iv} \in \mathbb{R}$ for robot i are given by:

$$\begin{aligned} \tilde{\boldsymbol{a}}_{if} &:= [\tilde{a}_{ifx} \; \tilde{a}_{ify}]^T = \hat{\boldsymbol{a}}_{if} - \boldsymbol{a}_{if}, \\ \tilde{a}_{iv} &= \hat{a}_{iv} - a_{iv}, \end{aligned} \tag{5}$$

We also denote the components of the velocity error of the system's center of mass by $s_x := \dot{x}_o - v_{des}$ and $s_y := \dot{y}_o$, and we define their integrals over time as:

$$\sigma_x = \int_o^t s_x d\tau, \qquad \sigma_y = \int_o^t s_y d\tau. \tag{6}$$

We define the following functions:

$$\begin{aligned} f_s(\theta_o) &= \sum_{i=1}^{N} ||\boldsymbol{r}_i|| \sin(\theta_o + \theta_i), \\ f_c(\theta_o) &= \sum_{i=1}^{N} ||\boldsymbol{r}_i|| \cos(\theta_o + \theta_i), \end{aligned} \tag{7}$$

$$\begin{aligned} \eta_{is} &= ||\boldsymbol{r}_i|| \int_o^t \sin(\theta_o + \theta_i)\dot{\theta}_o d\tau, \\ \eta_{ic} &= ||\boldsymbol{r}_i|| \int_o^t \cos(\theta_o + \theta_i)\dot{\theta}_o d\tau, \end{aligned} \tag{8}$$

$$\eta_s = \sum_{i=1}^{N} \eta_{is}, \qquad \eta_c = \sum_{i=1}^{N} \eta_{ic}, \tag{9}$$

$$\begin{aligned} \vartheta(\theta_o) = \sum_{i=1}^{n} ||\boldsymbol{r}_i|| \left(\eta_{is}\sin(\theta_o + \theta_i) + \eta_{ic}\cos(\theta_o + \theta_i)\right) \\ + \frac{\mu_v}{N} v_{des} f_s(\theta_o). \end{aligned} \tag{10}$$

Noting that $\dot{\theta}_o d\tau = d\theta_o$, the two integrals in Equation (8) can be calculated as:

$$\begin{aligned} \eta_{is} &= ||\boldsymbol{r}_i|| \left(\cos(\theta_o(0) + \theta_i) - \cos(\theta_o + \theta_i)\right), \\ \eta_{ic} &= ||\boldsymbol{r}_i|| \left(\sin(\theta_o + \theta_i) - \sin(\theta_o(0) + \theta_i)\right), \end{aligned} \tag{11}$$

where $\theta_o(0)$ is the initial orientation of the load. Henceforth, we will assume that $\theta_o(0) = 0$, without loss of generality.

By substituting Equation (11) into Equation (10), we can express $\vartheta(\theta_o)$ as:

$$\vartheta(\theta_o) = \rho^2 \sin(\theta_o) + \frac{\mu_v}{N} v_{des} f_s(\theta_o), \tag{12}$$

where

$$\rho = \left(\sum_{i=1}^{N} ||\boldsymbol{r}_i||^2\right)^{\frac{1}{2}}. \tag{13}$$

Since the second term on the right-hand side of Equation (12) is a sum of sine functions with different amplitudes and phases, this equation can be rewritten as:

$$\vartheta(\theta_o) = \rho^2 \sin(\theta_o) + b\sin(\theta_o + \beta), \tag{14}$$

in which b and β are constants that depend on $||\boldsymbol{r}_i||$ and θ_i, respectively, where $i = 1, ..., N$.

Substituting the control law Equation (3) into the system dynamics in Equation (2), and taking into account the kinematic relation between the robots' velocities and the payload's linear and angular velocities [4], the closed-loop dynamics of the system can be written as:

$$\begin{aligned} & m\ddot{\sigma}_x + c_t\dot{\sigma}_x + c_I\sigma_x - \kappa\dot{\eta}_s - \kappa_I\eta_s - \sum_{i=1}^{N}(\tilde{a}_{ifx} + \tilde{a}_{iv}\dot{x}_i) = 0, \\ & m\ddot{\sigma}_y + c_t\dot{\sigma}_y + c_I\sigma_y + \kappa\dot{\eta}_c + \kappa_I\eta_c - \sum_{i=1}^{N}(\tilde{a}_{ify} + \tilde{a}_{iv}\dot{y}_i) = 0, \\ & J\ddot{\theta}_o + c_r\dot{\theta}_o - \kappa f_s(\theta_o)\dot{\sigma}_x + \kappa f_c(\theta_o)\dot{\sigma}_y \\ & \quad - k_I(f_s(\theta_o)\sigma_x - f_c(\theta_o)\sigma_y) + k_I\vartheta(\theta_o) \\ & \quad + \sum_{i=1}^{N}(\tilde{a}_{ifx} + \tilde{a}_{iv}\dot{x}_i)||\boldsymbol{r}_i|| \sin(\theta_o + \theta_i) \\ & \quad - \sum_{i=1}^{N}(\tilde{a}_{ify} + \tilde{a}_{iv}\dot{y}_i)||\boldsymbol{r}_i|| \cos(\theta_o + \theta_i) = 0, \end{aligned} \tag{15}$$

in which the following are constant parameters:

$$\kappa = k - \frac{\mu_v}{N}, \quad \kappa_I = k_I - \frac{\mu_v}{N}, \quad r_g = \left(\frac{J}{m}\right)^{\frac{1}{2}},$$
$$c_t = kN, \quad c_I = k_I N, \quad c_r = \kappa\rho^2 + \mu_v r_g^2.$$

B. Adaptation Law

A *composite adaptation mechanism* is the combination of tracking-error-based (TEB) and prediction-error-based (PEB) adaptive laws [24]. For the TEB adaptive law, we can define the tracking errors as the robot velocity errors $\boldsymbol{s}_i$, $i = 1, ..., N$. The PEB adaptive law requires a linear relationship between the unknown parameters and variables that each robot can measure. Toward this end, we consider the model of power consumption by robot i as a basis to establish this linear model. Let E_i denote the mechanical energy of robot i, which consists only of kinetic energy since there is no potential field affecting the robots in this problem. Defining m_o as the mass of the load, m_r as the mass of each robot, and $m_i = m_r + \epsilon_{im} m_o$, where $\epsilon_{im} m_o$ is the fraction of the load mass that the robot carries, we have that $E_i = \frac{1}{2} m_i \dot{\boldsymbol{x}}_i^T \dot{\boldsymbol{x}}_i \in \mathbb{R}_{\geq 0}$. The time derivative of E_i can be written as:

$$\dot{E}_i = \boldsymbol{u}_i^T \dot{\boldsymbol{x}}_i - \boldsymbol{a}_{if}^T \dot{\boldsymbol{x}}_i - a_{iv} \dot{\boldsymbol{x}}_i^T \dot{\boldsymbol{x}}_i. \tag{16}$$

Since the rate of change in mechanical energy is the difference between the input power and the consumed power, we can identify the term $\boldsymbol{u}_i^T \dot{\boldsymbol{x}}_i$ as the input power to robot i, and the terms $\boldsymbol{a}_{if}^T \dot{\boldsymbol{x}}_i$ and $a_{iv} \dot{\boldsymbol{x}}_i^T \dot{\boldsymbol{x}}_i$ as the power consumed by Coulomb friction and viscous friction, respectively. The input power can be measured by the robot, since it is the dot product of the control torque and the robot's velocity. We express the input power in the following form, which is the matrix form of the above equation:

$$\boldsymbol{u}_i^T \dot{\boldsymbol{x}}_i = \boldsymbol{v}_i \boldsymbol{\Theta}_i, \tag{17}$$

in which $\boldsymbol{v}_i \in \mathbb{R}^{1\times 4}$ and $\boldsymbol{\Theta}_i \in \mathbb{R}^{4\times 1}$ are defined as:

$$\boldsymbol{v}_i = [\dot{x}_i \ddot{x}_i + \dot{y}_i \ddot{y}_i \quad \dot{x}_i \quad \dot{y}_i \quad \dot{x}_i^2 + \dot{y}_i^2],$$
$$\boldsymbol{\Theta}_i = [m_i \quad a_{ifx} \quad a_{ify} \quad a_{iv}]^T. \tag{18}$$

Since $\boldsymbol{v}_i$ contains the robot's acceleration, which can be a highly noisy measurement, we can use a filtered version of Equation (17) by applying a proper first-order filter such as $1/(s+\lambda)$ to the Laplace transform of both sides of the equation, where s is the complex angular frequency and λ is a positive real number [24]. We define ζ_i and $\boldsymbol{w}_i$ as the filtered versions of the input power and $\boldsymbol{v}_i$, respectively. Then, from Equation (17), the linear parametrization is given by:

$$\zeta_i = \boldsymbol{w}_i \boldsymbol{\Theta}_i. \tag{19}$$

The estimates of ζ_i and $\boldsymbol{\Theta}_i$ by robot i are denoted by $\hat{\zeta}_i$ and $\hat{\boldsymbol{\Theta}}_i$, respectively. We now can write the prediction error $e_i := \hat{\zeta}_i - \zeta_i$ as:

$$e_i = \boldsymbol{w}_i \hat{\boldsymbol{\Theta}}_i - \boldsymbol{w}_i \boldsymbol{\Theta}_i = \boldsymbol{w}_i \tilde{\boldsymbol{\Theta}}_i. \tag{20}$$

We propose the following composite adaptation law:

$$\dot{\hat{\boldsymbol{\Theta}}}_i = -\boldsymbol{\Gamma}(\boldsymbol{Y}_i^T \boldsymbol{s}_i + \boldsymbol{w}_i^T e_i), \tag{21}$$

in which $\boldsymbol{\Gamma} \in \mathbb{R}^{4\times 4}$ is a positive definite matrix that contains the adaptation gains, and $\boldsymbol{Y}_i \in \mathbb{R}^{2\times 4}$ is defined as:

$$\boldsymbol{Y}_i = [\boldsymbol{0}_{2\times 1} \quad \boldsymbol{I} \quad \dot{\boldsymbol{x}}_i]. \tag{22}$$

Remark 3.1: The control and adaptation laws in Equation (3) and Equation (21) are completely decentralized in the sense that they require only local measurements by each robot. From the expressions for $\boldsymbol{s}_i$, $\boldsymbol{Y}_i$, $\boldsymbol{w}_i$ and e_i, we see that each robot only needs its own velocity measurements to implement Equation (3) and Equation (21), and does not require information from its teammates or from a global supervisor.

IV. Stability and Convergence Analysis

To investigate the stability of the closed-loop dynamics in Equation (15), we consider the following Lyapunov function:

$$\begin{aligned} V &= \frac{1}{2} m(\dot{\sigma}_x^2 + \dot{\sigma}_y^2) + \frac{1}{2} J \dot{\theta}_o^2 + k_I b\,(1 - \cos(\theta_o + \beta)) \\ &+ \frac{1}{2} k_I \sum_{i=1}^{N} ((\sigma_x - \eta_{is})^2 + (\sigma_y + \eta_{ic})^2) \\ &+ \frac{1}{2} \sum_{i=1}^{N} \tilde{\boldsymbol{\Theta}}_i^T \boldsymbol{\Gamma}^{-1} \tilde{\boldsymbol{\Theta}}_i. \end{aligned} \tag{23}$$

Taking into account the adaptation law in Equation (21) and the fact that $\dot{\tilde{\boldsymbol{a}}}_{if} = \dot{\hat{\boldsymbol{a}}}_{if}$ and $\dot{\tilde{a}}_{iv} = \dot{\hat{a}}_{iv}$, the time derivative of this function is calculated as:

$$\begin{aligned} \dot{V} &= -c_t \dot{\sigma}_x^2 - c_I \sigma_x \dot{\sigma}_x + \kappa f_s \dot{\theta}_o \dot{\sigma}_x + k_I \dot{\sigma}_x \eta_s \\ &- c_t \dot{\sigma}_y^2 - c_I \sigma_y \dot{\sigma}_y - \kappa f_c \dot{\theta}_o \dot{\sigma}_y - k_I \dot{\sigma}_y \eta_c \\ &+ \dot{\sigma}_x \sum_{i=1}^{N} \tilde{a}_{ifx} + \dot{\sigma}_y \sum_{i=1}^{N} \tilde{a}_{ify} + \dot{\sigma}_x \sum_{i=1}^{N} \tilde{a}_{iv} \dot{x}_i + \dot{\sigma}_y \sum_{i=1}^{N} \tilde{a}_{iv} \dot{y}_i \\ &- c_r \dot{\theta}_o^2 + \kappa(f_s \dot{\sigma}_x - f_c \dot{\sigma}_y)\dot{\theta}_o + k_I (f_s \sigma_x - f_c \sigma_y)\dot{\theta}_o \\ &- k_I \rho^2 \sin(\theta_o)\dot{\theta}_o - k_I b \sin(\theta_o + \beta)\dot{\theta}_o + k_I b \dot{\theta}_o \sin(\theta_o + \beta) \\ &- \sum_{i=1}^{N} (\tilde{a}_{ifx} + \tilde{a}_{iv} \dot{x}_i)\dot{\eta}_{is} + \sum_{i=1}^{N} (\tilde{a}_{ify} + \tilde{a}_{iv} \dot{y}_i)\dot{\eta}_{ic} \\ &+ k_I \sum_{i=1}^{N} ((\sigma_x - \eta_{is})(\dot{\sigma}_x - \dot{\eta}_{is}) + (\sigma_y + \eta_{ic})(\dot{\sigma}_y + \dot{\eta}_{ic})) \\ &- \sum_{i=1}^{N} \tilde{\boldsymbol{a}}_{if}^T \boldsymbol{s}_i - \sum_{i=1}^{N} \tilde{a}_{iv}\,(\dot{x}_i(\dot{\sigma}_x - \dot{\eta}_{is}) + \dot{y}_i(\dot{\sigma}_y + \dot{\eta}_{ic})) \\ &- \sum_{i=1}^{N} \tilde{\boldsymbol{\Theta}}_i^T \boldsymbol{w}_i^T \boldsymbol{w}_i \tilde{\boldsymbol{\Theta}}_i. \end{aligned} \tag{24}$$

Given that $s_{ix} = \dot{\sigma}_x - \dot{\eta}_{is}$ and $s_{iy} = \dot{\sigma}_y + \dot{\eta}_{ic}$, we see that most of the terms in the expression above are canceled, and

$\dot{V}$ reduces to:

$$\dot{V} = -c_t\dot{\sigma}_x^2 - c_t\dot{\sigma}_y^2 - c_r\dot{\theta}_o^2 + 2\kappa\dot{\theta}_o(f_s\dot{\sigma}_x - f_c\dot{\sigma}_y) - \sum_{i=1}^{N} \tilde{\mathbf{\Theta}}_i^T \boldsymbol{w}_i^T \boldsymbol{w}_i \tilde{\mathbf{\Theta}}_i. \quad (25)$$

Defining $\boldsymbol{z} = [\dot{\sigma}_x \ \dot{\sigma}_y \ \dot{\theta}_o]^T$, we can write $\dot{V}$ in the following quadratic form:

$$\dot{V} = -\boldsymbol{z}^T\boldsymbol{Q}\boldsymbol{z} - \sum_{i=1}^{N} \tilde{\mathbf{\Theta}}_i^T \boldsymbol{w}_i^T \boldsymbol{w}_i \tilde{\mathbf{\Theta}}_i, \quad (26)$$

in which

$$\boldsymbol{Q} = \begin{bmatrix} c_t & 0 & \kappa f_s \\ 0 & c_t & -\kappa f_c \\ \kappa f_s & -\kappa f_c & c_r \end{bmatrix}. \quad (27)$$

As we proved in our previous work [4], $\boldsymbol{Q}$ is positive definite. Moreover, the second term in Equation (26) is quadratic in the estimation errors $\tilde{\mathbf{\Theta}}_i$. Thus, $\dot{V}$ is negative semi-definite, which implies the boundedness of V and the global stability of the closed-loop dynamics Equation (15), and consequently, the boundedness of σ_x, σ_y, $\dot{\sigma}_x$, $\dot{\sigma}_y$, $\dot{\theta}_o$, and $\tilde{\mathbf{\Theta}}_i$ for all $i \in \{1, 2, ..., N\}$. From Equation (3), this implies the boundedness of $\boldsymbol{u}_i$. Then, from the system dynamics in Equation (2), we can conclude the boundedness of $\ddot{\boldsymbol{q}}_o$, and therefore the boundedness of $\ddot{\sigma}_x$, $\ddot{\sigma}_y$ and $\ddot{\theta}_o$. Furthermore, using Equation (20), the second time derivative of V is calculated as:

$$\ddot{V} = -2\boldsymbol{z}^T\boldsymbol{Q}\dot{\boldsymbol{z}} - 2\sum_{i=1}^{N} e_i\dot{e}_i. \quad (28)$$

We can conclude that $\ddot{V}$ is bounded from: (1) the boundedness of $\boldsymbol{z}$ and $\dot{z} = [\ddot{\sigma}_x \ \ddot{\sigma}_y \ \ddot{\theta}_o]^T$, as discussed above; (2) the boundedness of e_i, which is immediately deduced from the boundedness of $\tilde{\mathbf{\Theta}}_i$ and $\boldsymbol{w}_i$, which contains the bounded velocities in $\dot{\boldsymbol{x}}_i$; and (3) the boundedness of $\dot{e}_i = \dot{\boldsymbol{w}}_i\tilde{\mathbf{\Theta}}_i + \boldsymbol{w}_i\dot{\tilde{\mathbf{\Theta}}}_i$, which is concluded from the exponential stability of the filter that was used to construct the linear parametrization Equation (19) and from the boundedness of the vectors and matrices in Equation (21). Since V is positive and $\ddot{V}$ is bounded, we can apply *Barbalat's lemma* [24] to conclude that $\dot{V} \to 0$, and consequently that $\boldsymbol{z} \to \mathbf{0}$ and $\tilde{\mathbf{\Theta}}_i \to \mathbf{0}$ as $t \to \infty$.

We now consider the first two equations in the closed-loop dynamics Equation (15). We see that when $\boldsymbol{z} = \mathbf{0}$ and $\tilde{\mathbf{\Theta}}_i = \mathbf{0}$, $i = 1, ..., N$, then $\sigma_x \equiv \eta_s$ and $\sigma_y \equiv -\eta_c$. Substituting $\sigma_x \equiv \eta_s$, $\sigma_y \equiv -\eta_c$ into the third equation of Equation (15), and using the trigonometric identity $\sin(a+b)+\sin(a-b) = 2\sin a \sin b$, we find that the following equation holds for $\theta_{o_{ss}}$, the steady-state value of θ_o:

$$b\sin(\theta_{o_{ss}} + \beta) - D\sin(\theta_{o_{ss}}) = 0, \quad (29)$$

where D is a constant defined as

$$D = 2\sum_{i=1}^{N}\sum_{j=i+1}^{N} ||\boldsymbol{r}_i||||\boldsymbol{r}_j|| \cos(\theta_i - \theta_j). \quad (30)$$

These two equations show that $\theta_{o_{ss}}$ depends on the distribution of the robots around the payload. (A comprehensive investigation of this relationship is beyond the scope of this paper, and is a topic of a future work.) In addition, since the constant b (when calculated explicitly) is inversely proportional to the number of robots, Equation (29) shows that $\theta_{o_{ss}}$ could be small with large teams of robots. Finally, because $\sigma_x \equiv \eta_s$ and $\sigma_y \equiv -\eta_c$, we see that the steady-state values of σ_x and σ_y are affected by $\theta_{o_{ss}}$ and the distribution of robots around the payload. From Equation (11), the norm of this error can be calculated as:

$$\sqrt{\sigma_x^2 + \sigma_y^2} = \sqrt{2\rho^2(1 - \cos(\theta_{o_{ss}}))}. \quad (31)$$

This norm is small when $\theta_{o_{ss}}$ is close to zero, which occurs when the team size is large, as mentioned above.

V. Simulation Results and Discussion

In this section, we validate our analysis with simulation results for collective transport by a team of point-mass (holonomic) robots that are rigidly attached to a rectangular payload. We illustrate the performance of the proposed controller and study the effect of the number of the robots on the system convergence to the target transport velocity, the amount of rotation exhibited by the load, and the translational drift of the load from the desired path in presence of Coulomb and viscous friction. The load is modeled as a homogeneous rectangle with mass $m_o = 1$ kg and moment of inertia $I_o = 0.4$ kg·m^2. The robots are identical, each with mass $m_r = 0.05$ kg. The controller gains are set to $k = 0.2$ and $k_I = 0.01$, and the target transport speed is $v_{des} = 0.1$ m/s. The target heading is set to $\gamma = \pi/6$ rad with respect to the x-axis of the inertial frame. The coefficients of Coulomb friction and viscous friction are defined as $\mu_f = 0.1$ and $\mu_v = 0.3$, respectively.

In the first simulation, the matrix of adaptation gains is set to $\Gamma = diag(0.6, 0.6, 0.6, 0.6)$, and the transport team consists of $N = 3$ robots, which are represented as colored circles in Figure 3. The figure shows that the robots transport the payload toward the goal along an oscillatory path. Figure 4 shows that the payload exhibits a slowly decaying rotational motion, and even though the angular velocity converges to zero, the payload still oscillates significantly during the transport. The rate of the payload's convergence to the desired velocity is very slow, and the payload ends at a drift of $d = 20$ cm from the desired path, and a total rotation of almost -30 degrees. Furthermore, the robots' estimates of the unknown parameter values converge to the final values very slowly, as shown in Figure 5.

In the second simulation, the number of robots is increased to $N = 6$, with the same matrix of adaptation gains. Figure 6 shows a significant improvement in the system's performance over the first simulation: the paths of the payload and the robots are much straighter, and after small initial fluctuations, they move on a straight line towards the goal. Moreover, as we can see in Figure 7, the payload's angular velocity and the velocity errors converge to zero very quickly, which results in the almost purely translational motion of the payload and

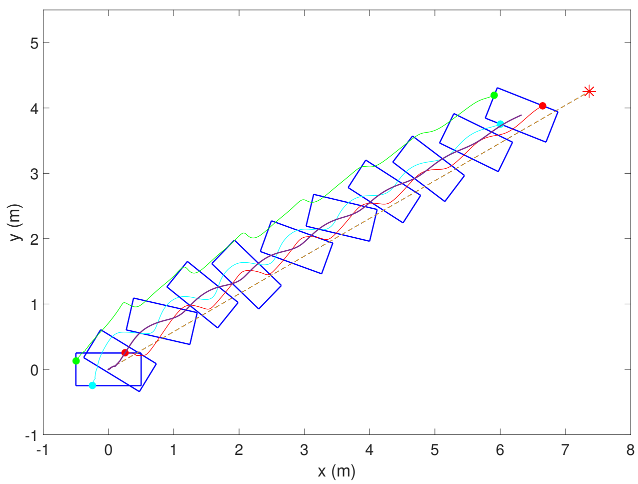

Fig. 3. Snapshots of a rectangular payload over time with $N = 3$ robots around its perimeter.

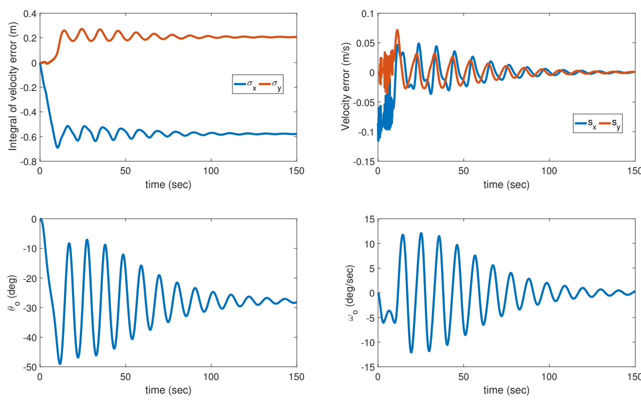

Fig. 4. Time evolution of the integral of the velocity error (σ_x and $\sigma_y = d$), the velocity error ($\dot{\sigma}_x = s_x$ and $\dot{\sigma}_y = s_y$), and the load's orientation θ_o and angular velocity $\omega_o = \dot{\theta}_o$ for the case of $N = 3$ robots.

a reduction in the amount of the drift from the original path to approximately $d = 3$ cm. Additionally, the robots' parameter estimates demonstrate smaller fluctuations and faster convergence to their final values.

VI. Conclusion

We have presented a decentralized adaptive control strategy for planar collective transport by a team of point-mass robots of a payload whose motion is disturbed by Coulomb and viscous frictional forces and moments. The controllers require only robots' measurements of their own velocities, and the only information provided to the robots is the target direction and speed of transport. The robots do not have any knowledge about the disturbance magnitudes and directions. We proved that the closed-loop system comprised of the payload and robots is globally stable, with velocity errors converging to zero and bounded estimation errors. We also studied the effect of the adaptation gain and the number of the robots on the payload's rate of convergence to the

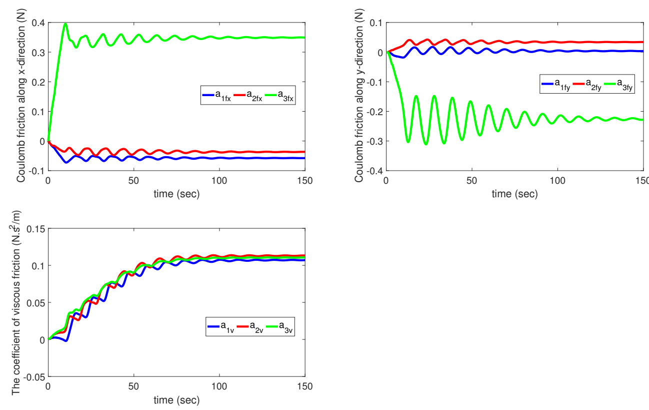

Fig. 5. Errors in each robot's estimates of the friction forces along the x and y directions, and the total errors $\tilde{a}_x$ and $\tilde{a}_y$, for the case of $N = 3$ robots.

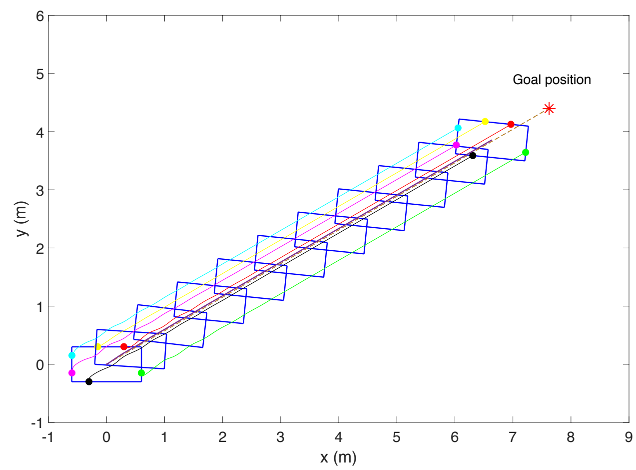

Fig. 6. Snapshots of a rectangular payload over time with $N = 6$ robots around its perimeter.

target transport velocity and drift from the desired path. Our simulations verified the correctness of our analysis for different adaptation gains and different team sizes.

In future work, we will design decentralized controllers for collective transport that implement autonomous obstacle avoidance for scenarios where the robots do not have prior information about the environment, and they must compute appropriate control commands based only on their measured distance from nearby obstacles within their sensing range. While [25] proposes decentralized controllers for this scenario, we will consider the additional restriction that the robots do not have feedback on the payload's motion. We will investigate the correctness and stability of a controller that combines the proposed adaptive controller with a repulsive component that is computed from local potential functions constructed by each robot. As illustrated by the preliminary simulation shown in Figure 9, this type of controller seems to yield promising results. We plan to establish theoretical guarantees on convergence, safety certificates, and local minima for this controller, and we will experimentally validate the controller with multi-robot experiments.

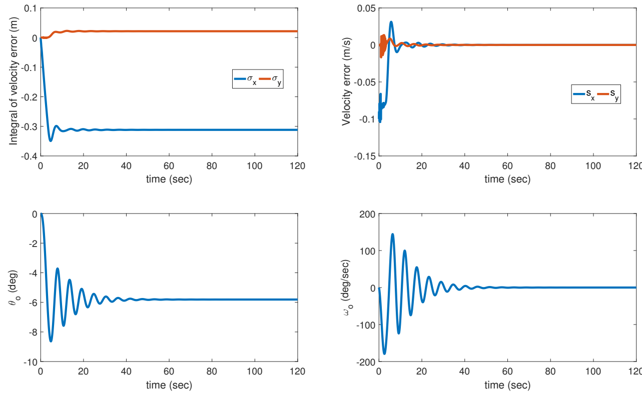

Fig. 7. Time evolution of the integral of the velocity error (σ_x and $\sigma_y = d$), the velocity error ($\dot{\sigma}_x = s_x$ and $\dot{\sigma}_y = s_y$), and the load's orientation θ_o and angular velocity $\omega_o = \dot{\theta}_o$ for the case of $N = 6$ robots.

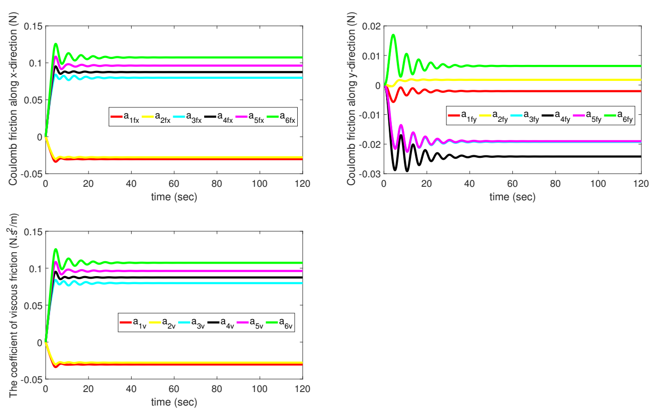

Fig. 8. Errors in each robot's estimates of the friction forces along the x and y directions, and the total errors $\tilde{a}_x$ and $\tilde{a}_y$, for the case of $N = 6$ robots.

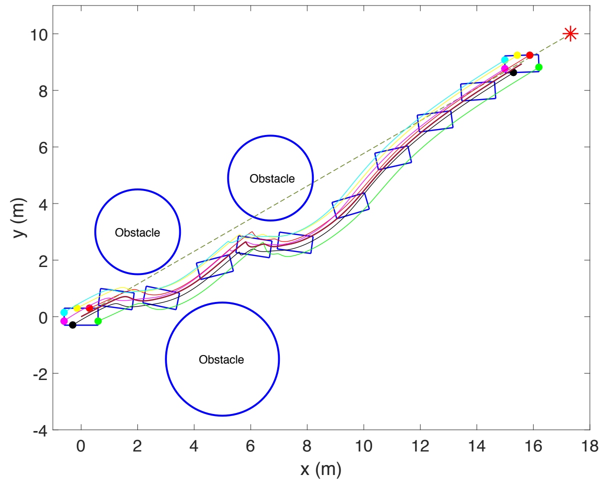

Fig. 9. Snapshots of a rectangular payload over time with six robots around its perimeter that perform collective transport while avoiding locally sensed obstacles.

References

[1] T. J. Czaczkes and F. L. Ratnieks, "Cooperative transport in ants (Hymenoptera: Formicidae) and elsewhere," *Myrmecological News*, vol. 18, pp. 1–11, 2013.

[2] H. F. McCreery and M. Breed, "Cooperative transport in ants: a review of proximate mechanisms," *Insectes Sociaux*, vol. 61, no. 2, pp. 99–110, 2014.

[3] A. Gelblum, I. Pinkoviezky, E. Fonio, N. S. Gov, and O. Feinerman, "Emergent oscillations assist obstacle negotiation during ant cooperative transport," *Proceedings of the National Academy of Sciences*, vol. 113, no. 51, pp. 14 615–14 620, 2016.

[4] H. Farivarnejad and S. Berman, "Stability and convergence analysis of a decentralized proportional-integral control strategy for collective transport," in *Proc. American Control Conference (ACC)*, June 2018, pp. 2794–2801.

[5] J. Chen, M. Gauci, W. Li, A. Kolling, and R. Groß, "Occlusion-based cooperative transport with a swarm of miniature mobile robots," *IEEE Transactions on Robotics*, vol. 31, no. 2, pp. 307–321, 2015.

[6] A. Franchi, A. Petitti, and A. Rizzo, "Distributed estimation of the inertial parameters of an unknown load via multi-robot manipulation," in *Proc. IEEE Int'l. Conf. on Decision and Control*, Dec 2014, pp. 6111–6116.

[7] A. Marino, G. Muscio, and F. Pierri, "Distributed cooperative object parameter estimation and manipulation without explicit communication," in *Proc. IEEE Int'l. Conf. on Robotics and Automation (ICRA)*, May 2017, pp. 2110–21 116.

[8] L. Jin, S. Li, X. Luo, Y. Li, and B. Qin, "Neural dynamics for cooperative control of redundant robot manipulators," *IEEE Transactions on Industrial Informatics*, vol. PP, no. 99, pp. 1–1, 2018.

[9] A. Marino and F. Pierri, "A two stage approach for distributed cooperative manipulation of an unknown object without explicit communication and unknown number of robots," *Robotics and Autonomous Systems*, vol. 103, pp. 122 – 133, 2018.

[10] A. Tsiamis, C. K. Verginis, C. P. Bechlioulis, and K. J. Kyriakopoulos, "Cooperative manipulation exploiting only implicit communication," in *Proc. IEEE/RSJ Int'l. Conf. on Intelligent Robots and Systems (IROS)*, Sept 2015, pp. 864–869.

[11] W. Gueaieb, F. Karray, and S. Al-Sharhan, "A robust adaptive fuzzy position/force control scheme for cooperative manipulators," *IEEE Transactions on Control Systems Technology*, vol. 11, no. 4, pp. 516–528, July 2003.

[12] Z. Li, C. Yang, C. Y. Su, S. Deng, F. Sun, and W. Zhang, "Decentralized fuzzy control of multiple cooperating robotic manipulators with impedance interaction," *IEEE Transactions on Fuzzy Systems*, vol. 23, no. 4, pp. 1044–1056, Aug 2015.

[13] H. Bai and J. T. Wen, "Cooperative load transport: A formation-control perspective," *IEEE Transactions on Robotics*, vol. 26, no. 4, pp. 742–750, Aug 2010.

[14] S. Kim, H. Seo, J. Shin, and H. J. Kim, "Cooperative aerial manipulation using multirotors with multi-dof robotic arms," *IEEE/ASME Transactions on Mechatronics*, vol. PP, no. 99, pp. 1–1, 2018.

[15] H. Lee, H. Kim, W. Kim, and H. J. Kim, "An integrated framework for cooperative aerial manipulators in unknown environments," *IEEE Robotics and Automation Letters*, vol. PP, no. 99, pp. 1–1, 2018.

[16] N. Sadati and A. Ghaffarkhah, "Decentralized position and force control of nonredundant multi-manipulator systems," in *Proc. Int'l. Conf. on Control, Automation and Systems*, Oct 2007, pp. 2223–2229.

[17] G. B. Dai and Y. C. Liu, "Distributed coordination and cooperation control for networked mobile manipulators," *IEEE Transactions on Industrial Electronics*, vol. 64, no. 6, pp. 5065–5074, June 2017.

[18] H. Lee, H. Kim, and H. J. Kim, "Planning and control for collision-free cooperative aerial transportation," *IEEE Transactions on Automation Science and Engineering*, vol. PP, no. 99, pp. 1–13, 2017.

[19] A. Marino, "Distributed adaptive control of networked cooperative mobile manipulators," *IEEE Transactions on Control Systems Technology*, vol. PP, no. 99, pp. 1–15, 2017.

[20] J. Pliego-Jimenez and M. Arteaga-Perez, "On the adaptive control of cooperative robots with time-variant holonomic constraints," *International Journal of Adaptive Control and Signal Processing*, vol. 31, no. 8, pp. 1217–1231, 2017.

[21] P. Culbertson and M. Schwager, "Decentralized adaptive control for collaborative manipulation," in *Proc. IEEE Int'l. Conf. on Robotics and Automation (ICRA)*, May 2018.

[22] H. Farivarnejad, S. Wilson, and S. Berman, "Decentralized sliding

mode control for autonomous collective transport by multi-robot systems," in *IEEE Int'l. Conf. on Decision and Control (CDC)*, Dec 2016, pp. 1826–1833.

[23] Z. Wang and M. Schwager, "Multi-robot manipulation without communication," in *Proc. Int'l. Symposium on Distributed Autonomous Robotic Systems (DARS)*, Nov. 2014, pp. 43–56.

[24] J.-J. E. Slotine and W. Li, *Applied Nonlinear Control*. Englewood Cliffs, N.J.: Prentice Hall, 1991.

[25] S. G. Faal, S. T. Kalat, and C. D. Onal, "Decentralized obstacle avoidance in collective object manipulation," in *Proc. NASA/ESA Conference on Adaptive Hardware and Systems (AHS)*, July 2017, pp. 133–138.

View publication stats